Supporting Information

# Enhanced Thermal Conductivity and Reduced Thermal Resistance in Carbon Fiber-based Thermal Interface Materials with Vertically Aligned Structure

Zhenbang Zhang[a,b], Rongjie Yang[a], Yandong Wang[a], Kang Xu[a], Wen Dai[a], Jianxiang Zhang[a], Maohua Li[a], Linhong Li[a], Yingying Guo[a], Yue Qin[a], Boda Zhu[a], Yiwei Zhou[a], Xingye Wang[a], Tao Cai[a,c], Cheng-Te Lin[a,c], Kazuhito Nishimura[a,c], Hao Nan Li[b,] *, Nan Jiang[a,c,] *and Jinhong Yu[a,c,] *

[a] Key Laboratory of Marine Materials and Related Technologies, Zhejiang Key Laboratory of Marine Materials and Protective Technologies, Ningbo Institute of Materials Technology and Engineering, Chinese Academy of Sciences, Ningbo 315201, China

[b] Nottingham Ningbo China Beacons of Excellence Research and Innovation Institute, University of Nottingham Ningbo China,

[c] Center of Materials Science and Optoelectronics Engineering, University of Chinese Academy of Sciences, Beijing 100049, China
*Corresponding author. E-mail: yujinhong@nimte.ac.cn

**This file includes:**

**Supplementary Figures**

## Supplementary Tables

**Supplementary Figures and Tables**

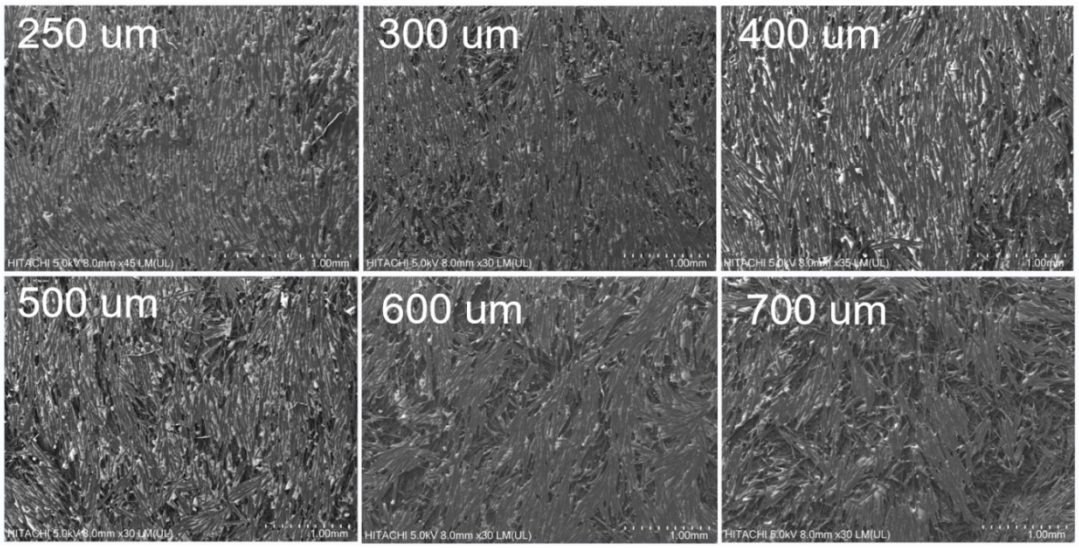


**Figure S1** Microstructure of various rolling thickness of single layer of composite with 73.68 wt% filler loading in top view.

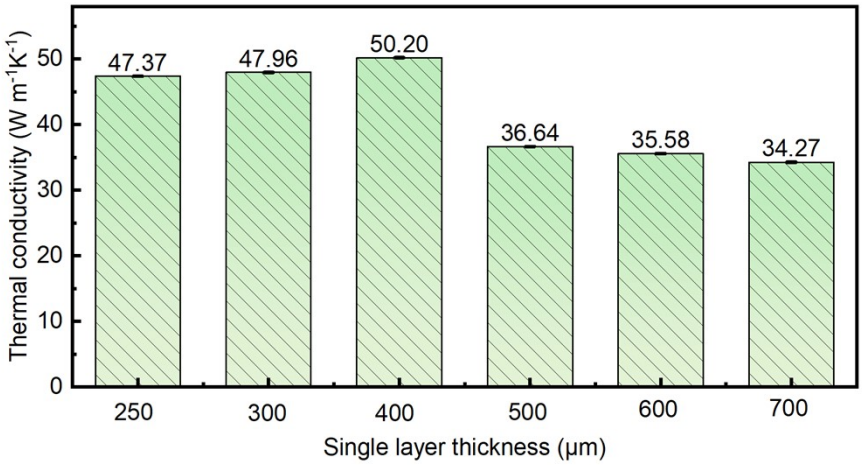


**Figure S2** Effect of rolling thickness of single layer of composite on thermal conductivity for VCB-73.68 wt% -X.

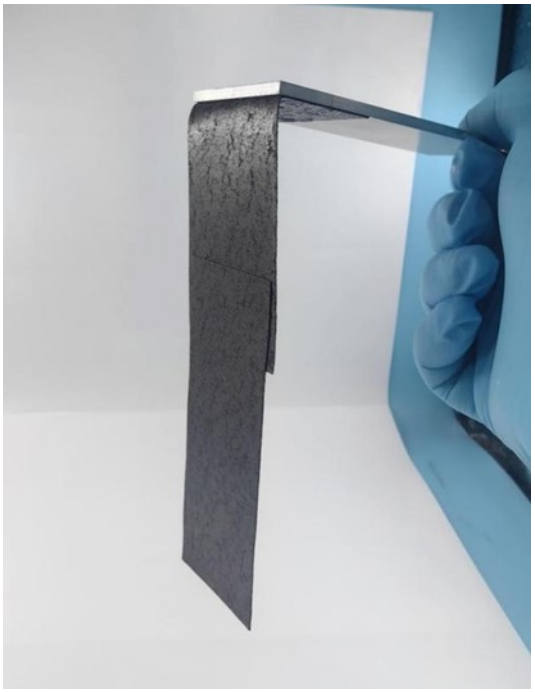

**Figure S3** Adhesion test of VCB composite.

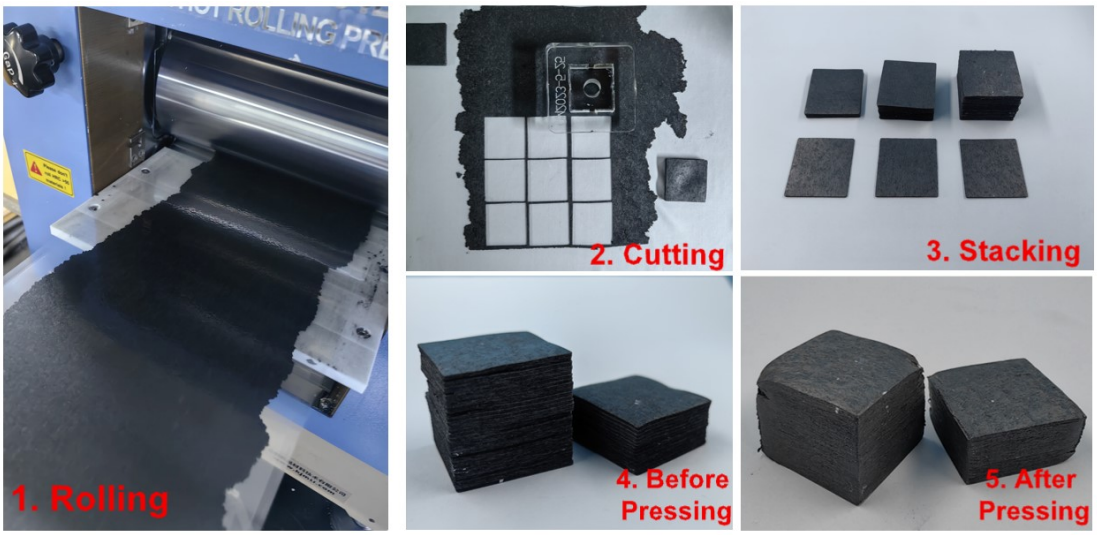


**Figure S4** Preparation process of VCB composites and corresponding photos.

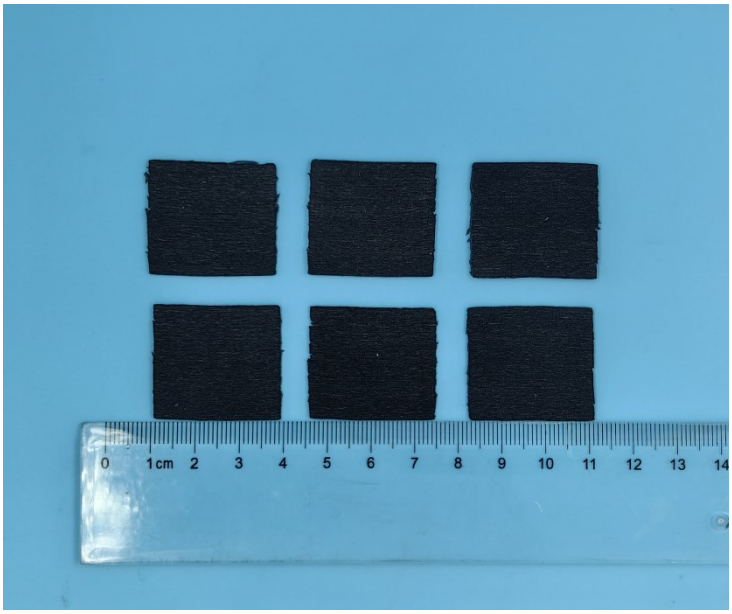


**Figure S5** Optical photography of the VCB composite after sclicing.

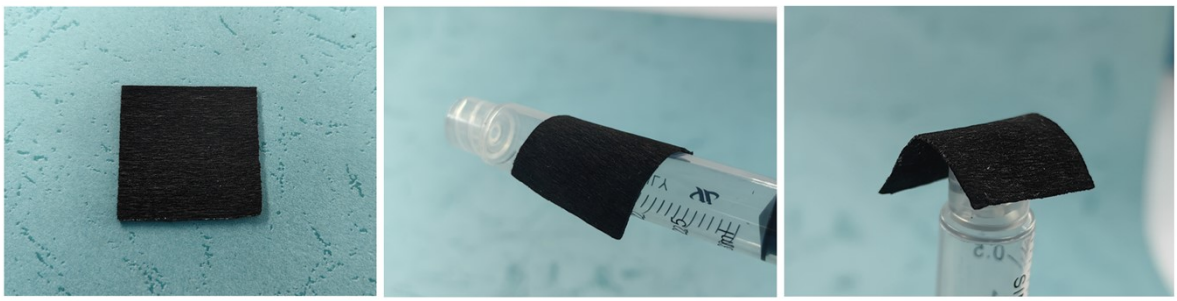

**Figure S6.**Photographs of VCB composite in flat and bent states.

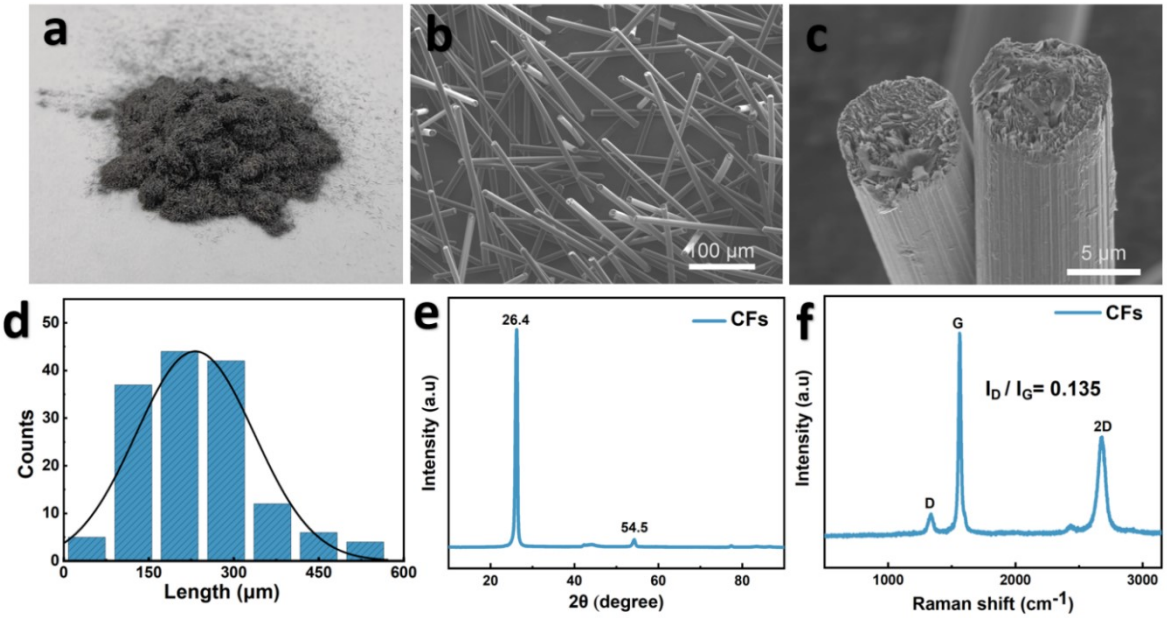


**Figure S7** Characterization of carbon fiber (CF). (a) Opticial photography of CF. (b) SEM image of CF. (c) Microstructure of CF in cross-section view. (d) Statistical diagram of length distribution for CF. (e) XRD pattern of CF. (f) Raman spectrum of CF.

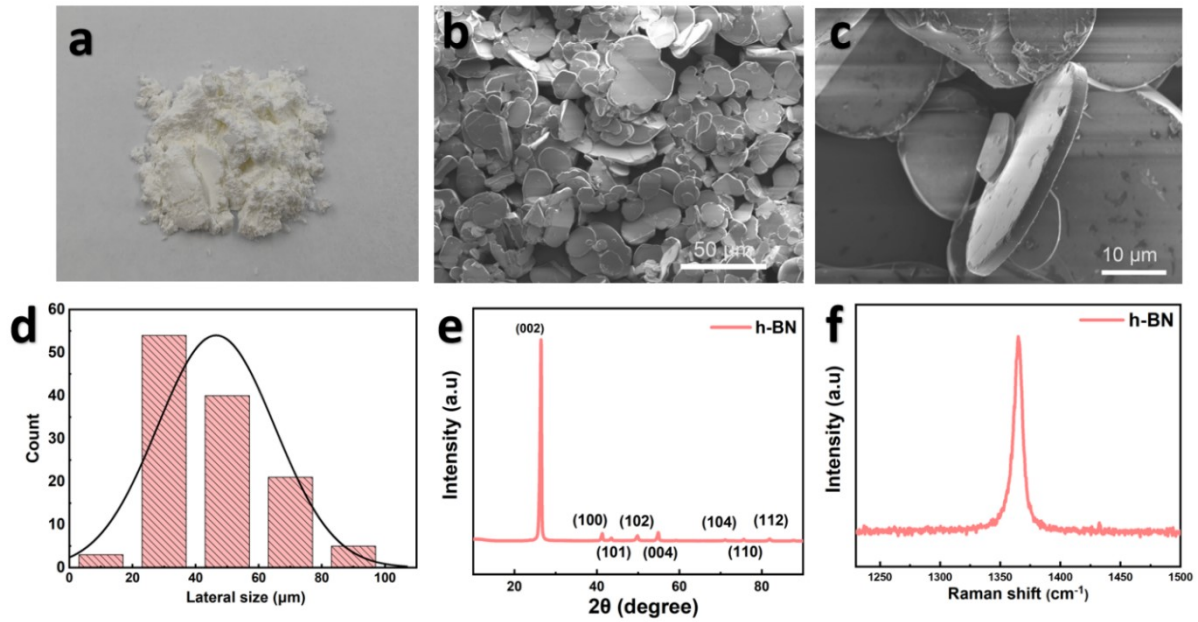


**Figure S8** Characterization of hexagonal boron nitride (BN). (a) Opticial photography of BN. (b-c) SEM image of BN. (d) Statistical diagram of lateral size distribution for BN. (e) XRD pattern of BN. (f) Raman spectrum of BN.

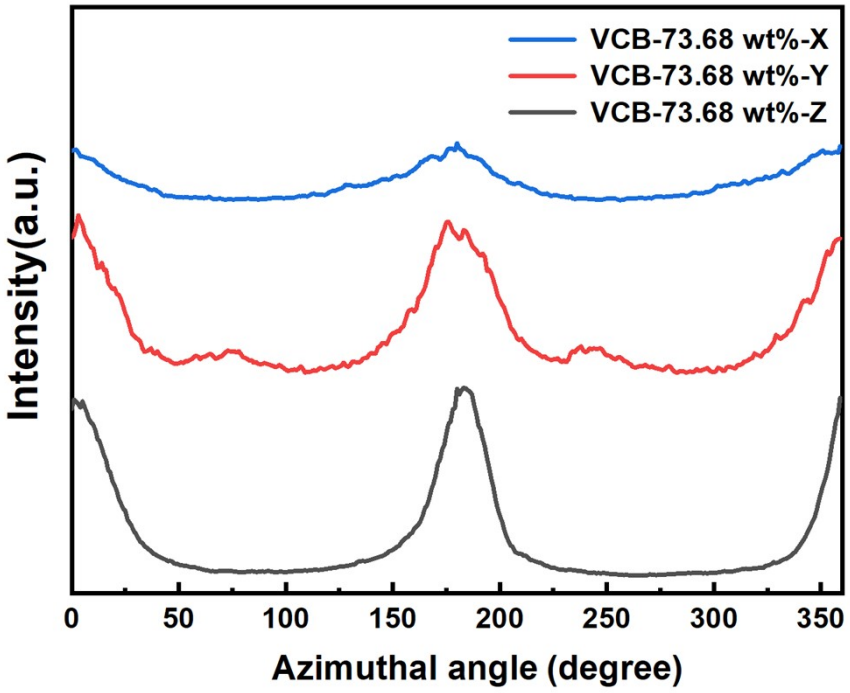


**Figure S9** Integral intensity of (002) crystal vs azimuth angle curves of VCB-73.68 wt%-X, VCB-73.68 wt%-Y and VCB-73.68 wt%-Z.

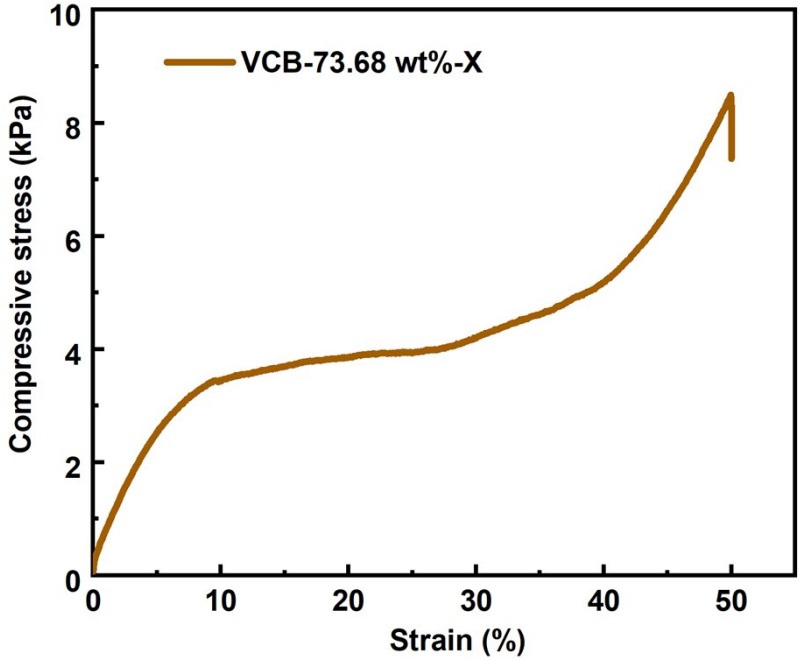


**Figure S10** Compression stress-strain curve of VCB-73.68 wt%-X.

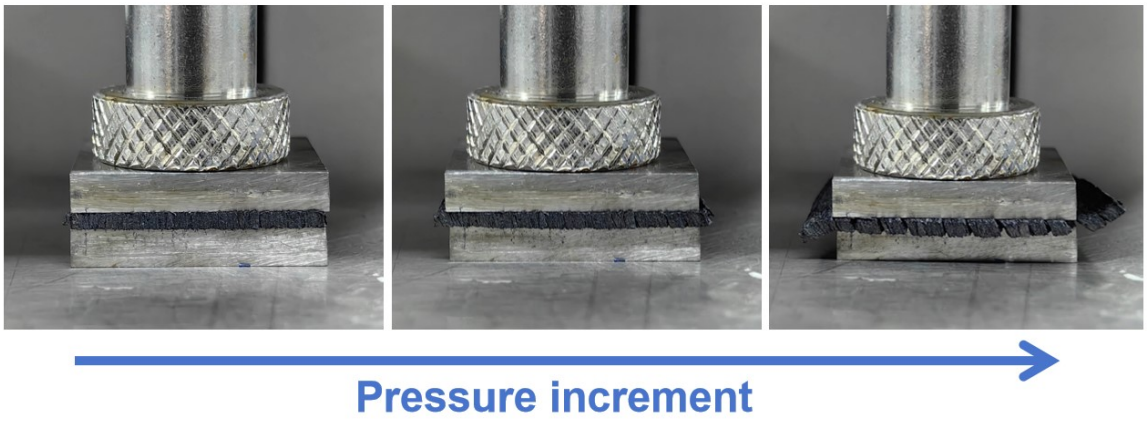


**Figure S11** Deformation of VCB composites with increasing pressure.

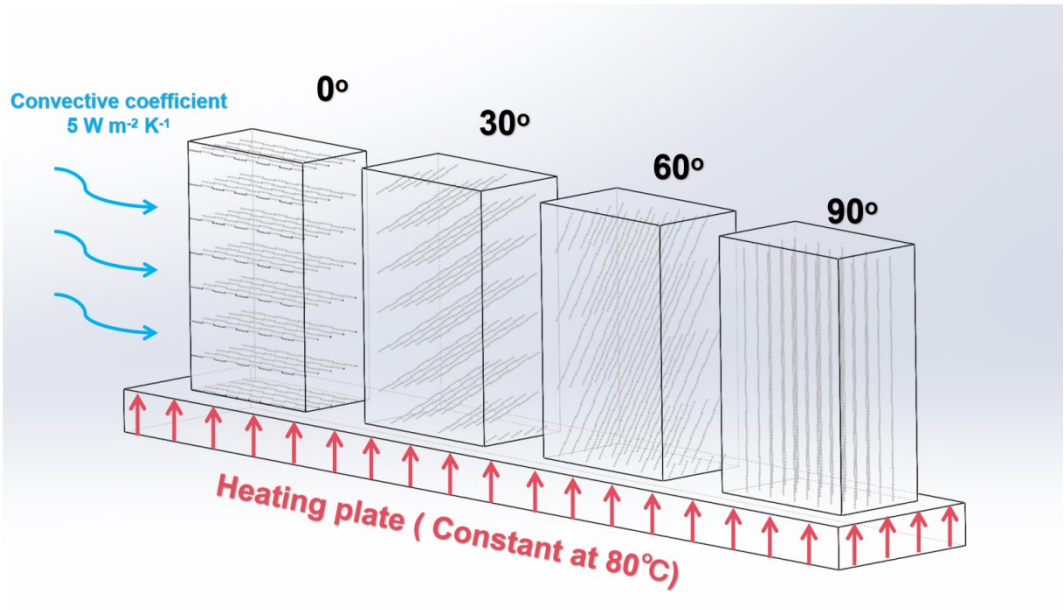


**Figure S12** Schematic of the ANSYS simulation models and the boundary conditions.

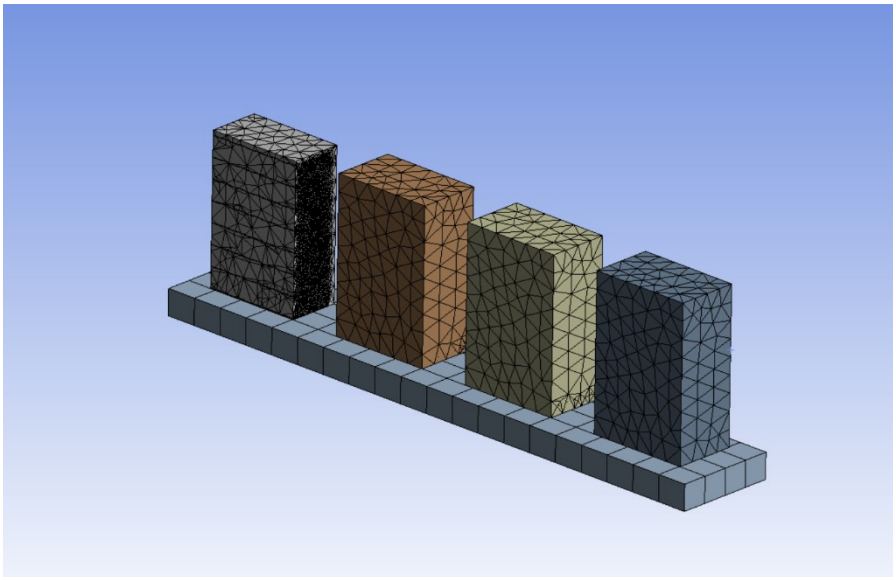

**Figure S13** Schematic of the ANSYS simulation meshing models.

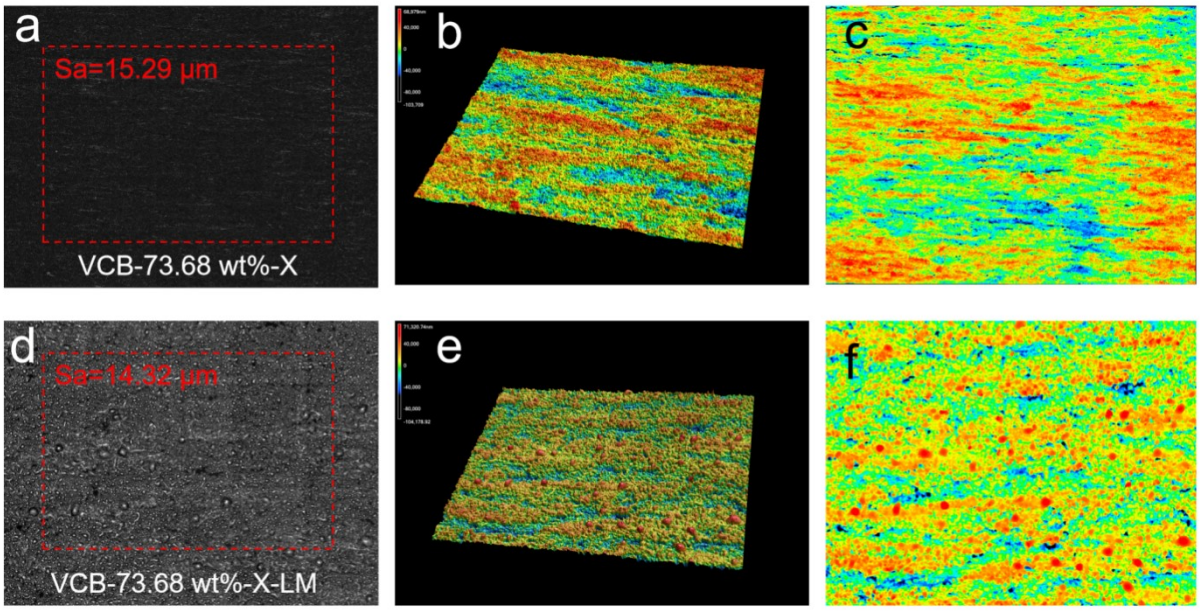


**Figure S14** Surface topography of VCB -73.68 wt%-X and VCB -73.68 wt%-X-LM.

Table S1 The parameters for calculating the through-plane thermal conductivity of PDMS and the VCB composites.

| Sample | Thermal diffusivity ($mm^2 s^{-1}$) | Specific heat capacity ($J g^{-1} K^{-1}$) | Density ($g cm^{-3}$) | Thermal conductivity ($W m^{-1} K^{-1}$) |
|---|---|---|---|---|
| PDMS | 0.11 | 1.52 | 1.03 | 0.16 |
| VCB-55 wt%-X | 18.09 ± 0.23 | | | 25.67 ± 0.32 |
| VCB-55 wt%-Y | 6.13 ± 0.21 | 1.10 | 1.29 | 8.71 ± 0.29 |
| VCB-55 wt%-Z | 1.10 ± 0.01 | | | 1.55 ± 0.01 |
| VCB-60 wt%-X | 19.07 ± 0.84 | | | 27.13 ± 1.20 |
| VCB-60 wt%-Y | 7.41 ± 0.21 | 1.07 | 1.33 | 10.54 ± 0.30 |
| VCB-60 wt%-Z | 1.13 ± 0.01 | | | 1.61 ± 0.01 |
| VCB-65 wt%-X | 22.98 ± 1.07 | | | 32.82 ± 1.53 |
| VCB-65 wt%-Y | 8.28 ± 0.33 | 1.05 | 1.36 | 11.83 ± 0.47 |
| VCB-65 wt%-Z | 1.28 ± 0.01 | | | 1.83 ± 0.01 |
| VCB-70 wt%-X | 26.84 ± 0.28 | | | 39.08 ± 0.41 |
| VCB-70 wt%-Y | 9.87 ± 0.36 | 1.04 | 1.40 | 14.37 ± 0.53 |
| VCB-70 wt%-Z | 1.30 ± 0.01 | | | 1.87 ± 0.01 |
| VCB-73.68 wt%-X | 35.48 ± 1.10 | | | 51.90 ± 1.62 |
| VCB-73.68 wt%-Y | 11.84 ± 1.04 | 1.03 | 1.42 | 17.32 ± 1.53 |
| VCB-73.68 wt%-Z | 1.42 ± 0.01 | | | 2.07 ± 0.01 |

Table S2 Comparison of thermal conductivity of our VCB composites with reported others CFs-TIMs.

| No. | Alignment technology | CF type | Matrix | Filler | Loading | K ($Wm^{-1} K^{-1}$) | Ref. |
|---|---|---|---|---|---|---|---|
| 1 | Ice template | Milled fiber | Epoxy | CF | 13 vol% | 2.82 | [1] |
| 2 | Ice template | Milled fiber | PDMS | CF | 12.8 wt% | 6.04 | [2] |
| 3 | Ice template | Milled fiber | Epoxy | CF | 30.52 wt% | 9.68 | [3] |
| 4 | Electrostatic flocking | Milled fiber | Silicone rubber | CF-CNT | 4.01 wt% | 8.92 | [4] |
| 5 | Electrostatic flocking | Milled fiber | AB resin | CF | 13.4 wt% | 15.3 | [5] |
| 6 | Electrostatic flocking | Milled fiber | FKM | CF | 13.2 wt% | 23.3 | [6] |
| 7 | Magnetic | Milled fiber | Silicone rubber | CFs | 9 vol% | 4.72 | [7] |
| 8 | Magnetic | Milled fiber | silicone rubber | CF/ $Al_2O_3$ | 20 vol%/ 20 vol% | 26.49 | [8] |
| 9 | Magnetic | Milled fiber | PDMS | CF | 47.3 wt% | 45.01 | [9] |
| 10 | 3D printing | Milled fiber | PDMS | CF/ $Al_2O_3$ | 12.1 wt%/ 78.8 wt% | 21.29 | [10] |
| 11 | 3D printing | Milled fiber | PDMS | CFs | 60 wt% | 35.22 | [11] |
| 12 | 3D printing | Milled fiber | PDMS | CF/ $Al_2O_3$ | 24 vol%/ 47 vol% | 38 | [12] |
| 13 | Pressing | Continuous fiber | OBC | CF | 20 wt% | 5.63 | [13] |
| 14 | Pre-array | Continuous fiber | PDMS | NiCO@ | 53.28 wt% | 15.55 | [14] |
| | | | | CFs | 44.46 wt% | 34.94 | |
| 15 | Pre-array | Continuous fiber | PDMS | CF | 20 vol% | 43.47 | [15] |
| 16 | Pie-Rolling | Milled fiber | PDMS | CF/Al | 10.6wt%/ 74.4 wt% | 10.46 | [16] |
| 17 | Press-Rolling | Milled fiber | PDMS | CF/BN | 73.68 wt% | 51.9 | This work |

Table S3 Comparison of thermal conductivity and density between composites with carbon fiber-based, BN-based, and commercial TIMs as reported in the literature.

| No. | Type | Matrix | Filler | Filler loading | K ($W \cdot m^{-1} \cdot K^{-1}$) | ρ ($g \cdot cm^{-3}$) | Ref |
|---|---|---|---|---|---|---|---|
| 1 | CF based | OBC | CF | 30 vol% | 15.01 | 1.266 | [17] |
| 2 | | OBC/Paraffin wax | CF | 20 wt% | 5.63 | 1.03 | [13] |
| 3 | | Epoxy | CF | 49 wt% | 32.12 | 1.48 | [18] |
| 4 | | PDMS | CF | 46.9 wt% | 45.01 | 1.373 | [9] |
| 5 | BN based | Epoxy | BN flake/BN sphere | 50 wt% | 4.27 | 1.24 | [19] |
| 6 | | PDMS | BN | 27.05 vol% | 5.134 | 1.534 | [20] |
| 7 | | PTFE | BNNS | 30 wt% | 1.28 | 2.1 | [21] |
| 8 | | PU | BNNS | 80 vol% | 11.5 | 1.77 | [22] |
| 9 | | PVP | BN | 62.6 vol% | 12.1 | 1.3 | [23] |
| 10 | Commercial | Silicone rubber | CF | - | 40 | 2.4 | Dexerials，EX20000C4S |
| 11 | | Silicone rubber | CF | - | 35 | 2.2 | Dexerials，EX20000C9S |
| 12 | | Silicone rubber | CF | - | 30 | 2.4 | Dexerials，EX10000F7 |
| 13 | | Silicone rubber | CF | - | 25 | 2.6 | Waretimo，WT5935C-250-65 |
| 14 | | Silicone rubber | CF | - | 25 | 3.3 | T-Globa，TG-AH25 |
| 15 | CF based | PDMS | CF | 73.68 wt% | 51.9 | 1.42 | This work |

Table S4 Comparison of total thermal resistance and thermal conductivity between VCB-73.68 wt%-X-LM and TIMs which reported in the literature.

| No. | Type | Matrix | Filler | Filler loading | Temperature (℃) | Pressure | Thermal resistence ($K \cdot cm^2 \cdot W^{-1}$) | K ($W \cdot m^{-1} \cdot K^{-1}$) | Ref. |
|---|---|---|---|---|---|---|---|---|---|
| 1 | Grease | Silicone oil | Graphene/ alumina | 72 wt% | 80 | 60 Psi | 0.243 | 4.38 | [24] |
| 2 | Grease | Silicone oil | AlN | 74.8 wt% | - | 50 Psi | 0.962 | 1.55 | [25] |
| 3 | PCM hydrogel | PEG | Graphene | 7 wt% | 80 | 50 psi | 0.5 | 1.23 | [26] |
| 4 | PCM hydrogel | OP | Ag flake/ nAgMWNT | 46 vol%/2.5 vol% | 40 | 3 Mpa | 0.305 | 43.4 | [27] |
| 5 | Thermal Pad | Silicone ruber | Graphite/ carbon fiber | - | 80 | 30 Psi | 1.8 | 19.1 | [28] |
| 6 | Thermal Pad | PDMS | Carbon fiber | 20 vol% | - | 20 Psi | 0.6 | 43.47 | [15] |
| 7 | Thermal Pad | Silicone ruber | BN | 64.3 wt% | - | 0.69 Mpa | 0.39 | 1.01 | [29] |
| 8 | Thermal Pad | PDMS | BN/LM | 50 Vol% | | 18 Psi | 2.53 | 3.2 | [30] |
| 9 | Thermal Pad | PDMS | Diamond /LM | 89.1 wt% | | 560 Kpa | 0.38 | 29 | [31] |
| 10 | Thermal Pad | PDMS | Carbon fiber/BN | 73.68 wt% | 80 | 100 Psi | 0.26 | 51.9 | This work |

## Supplementary References


1. J. Ma, T. Shang, L. Ren, Y. Yao, T. Zhang, J. Xie, B. Zhang, X. Zeng, R. Sun, J.-B. Xu and C.-P. Wong, *Chemical Engineering Journal*, 2020, **380**, 122550.
2. X. Hou, Y. Chen, W. Dai, Z. Wang, H. Li, C.-T. Lin, K. Nishimura, N. Jiang and J. Yu, *Chemical Engineering Journal*, 2019, **375**, 121921.
3. L. Guo, Z. Zhang, M. Li, R. Kang, Y. Chen, G. Song, S.-T. Han, C.-T. Lin, N. Jiang and J. Yu, *Composites Communications*, 2020, **19**, 134-141.
4. T. Ji, Y. Feng, M. Qin, S. Li, F. Zhang, F. Lv and W. Feng, *Carbon*, 2018, **131**, 149-159.
5. Z. Yu, S. Wei and J. Guo, *Journal of Materials Science: Materials in Electronics*, 2019, **30**, 10233-10243.
6. K. Uetani, S. Ata, S. Tomonoh, T. Yamada, M. Yumura and K. Hata, *Advanced Materials*, 2014, **26**, 5857-5862.
7. D. Ding, R. Huang, X. Wang, S. Zhang, Y. Wu, X.-a. Zhang, G. Qin, Z. Liu, Q. Zhang and Y. Chen, *Chemical Engineering Journal*, 2022, **441**, 136104.
8. Q. Wu, W. Li, C. Liu, Y. Xu, G. Li, H. Zhang, J. Huang and J. Miao, *Carbon*, 2022, **187**, 432-438.
9. S. Han, Y. Ji, Q. Zhang, H. Wu, S. Guo, J. Qiu and F. Zhang, *Nano-Micro Letters*, 2023, **15**, 146.
10. F. Huang, W. Qin, D. Shu, J. Sun, J. Li, D. Meng, W. Yue and C. Wang, *Ceramics International*, 2023, **49**, 32971-32978.
11. Z. Zhang, M. Li, Y. Wang, W. Dai, L. Li, Y. Chen, X. Kong, K. Xu, R. Yang, P. Gong, J. Zhang, T. Cai, C.-T. Lin, K. Nishimura, H. N. Li, N. Jiang and J. Yu, *Journal of Materials Chemistry A*, 2023, **11**, 10971-10983.
12. R. Huang, D. Ding, X. Guo, C. Liu, X. Li, G. Jiang, Y. Zhang, Y. Chen, W. Cai and X.-a. Zhang, *Composites Science and Technology*, 2022, **230**, 109717.
13. P. Zhang, Y. Qiu, C. Ye and Q. Li, *Chemical Engineering Journal*, 2023, **461**, 141940.
14. Z. Zhang, J. Wang, J. Shang, Y. Xu, Y. J. Wan, Z. Lin, R. Sun and Y. Hu, *Small*, 2023, **19**, e2205716.
15. J. Li, Z. Ye, P. Mo, Y. Pang, E. Gao, C. Zhang, G. Du, R. Sun and X. Zeng, *Composites Science and Technology*, 2023, **234**, 109948.
16. T. Jiao, B. Han, L. Zhao, Z. Zhang, Y. Zeng, D. Li, K. Zhang, Q. Deng, Y. Zhao and Z. Li, *Applied Surface Science*, 2023, **618**, 156711.
17. G. Zhang, S. Xue, F. Chen and Q. Fu, *Composites Science and Technology*, 2023, **231**, 109784.
18. M. Li, Z. Ali, X. Wei, L. Li, G. Song, X. Hou, H. Do, J. C. Greer, Z. Pan, C.-T. Lin, N. Jiang and J. Yu, *Composites Part B: Engineering*, 2021, **208**, 108599.
19. W. Jang, S. Lee, N. R. Kim, H. Koo, J. Yu and C.-M. Yang, *Composites Part B: Engineering*, 2023, **248**, 110355.
20. C. Lei, Y. Zhang, D. Liu, X. Xu, K. Wu and Q. Fu, *Composites Science and Technology*, 2021, **214**, 108995.
21. L. Xu, K. Zhan, S. Ding, J. Zhu, M. Liu, W. Fan, P. Duan, K. Luo, B. Ding, B. Liu, Y. Liu, H. M. Cheng and L. Qiu, *ACS Nano*, 2023, **17**, 4886-4895.
22. N. Zhao, J. Li, W. Wang, W. Gao and H. Bai, *ACS Nano*, 2022, **16**, 18959-18967.
23. H. He, W. Peng, J. Liu, X. Y. Chan, S. Liu, L. Lu and H. Le Ferrand, *Advanced Materials*, 2022, **34**, e2205120.
24. C. Chen, Y. He, C. Liu, H. Xie and W. Yu, *Journal of Materials Science: Materials in Electronics*, 2020, **31**, 4642-4649.
25. P. Luo, Y. Tuersun, X. Huang, H. Yang and S. Chu, *Advanced Engineering Materials*, 2023, **25**, 2301092.
26. J. Yang, W. Yu, C. Liu, H. Xie and H. Xu, *Composites Science and Technology*, 2022,

**219**, 109223.
27. S. A. Abdul Jaleel, T. Kim and S. Baik, *Advanced Materials*, 2023, **35**, e2300956.
28. M. Li, L. Li, X. Hou, Y. Qin, G. Song, X. Wei, X. Kong, Z. Zhang, H. Do, J. C. Greer, F. Han, T. Cai, W. Dai, C.-T. Lin, N. Jiang and J. Yu, *Composites Science and Technology*, 2021, **212**.
29. Y. Ji, S.-D. Han, H. Wu, S.-Y. Guo, F.-S. Zhang and J.-H. Qiu, *Chinese Journal of Polymer Science*, 2023, DOI: 10.1007/s10118-023-3023-2.
30. Z. Wang, J. Li, N. Ye, H. Zhang, D. Yang and Y. Lu, *Composites Science and Technology*, 2023, **233**, 109903.
31. S. Wei, W. Wang, L. Zhou and J. Guo, *Composites Part A: Applied Science and Manufacturing*, 2022, **162**, 107149.